Pergamon

Int. J. Solids Structures Vol. 32, No. 19, pp. 2835–2852, 1995

0020-7683/95 $9.50 + .00

0020-7683(94)00269-X

AUGMENTED HOOKE'S LAW IN FREQUENCY DOMAIN. A THREE DIMENSIONAL, MATERIAL DAMPING FORMULATION

K. DOVSTAM
The Aeronautical Research Institute of Sweden, P.O. Box 11021, S-161 11 Bromma, Sweden

(*Received* 5 *May* 1994; *in revised form* 14 *November* 1994)

Abstract—An isothermal, fully three-dimensional material damping modelling technique, to some extent alternative to classic viscoelasticity, is proposed. The method is formulated in the frequency domain as an augmented Hooke's law (AHL) with a constitutive matrix in which material damping is introduced by adding frequency dependent, complex valued terms to the classical material modulus matrix of Hooke's generalized law. The derivations are based on linear, irreversible thermodynamics and the concept of hidden coordinates as introduced by Biot [(1955) *Phys. Rev.* **97**, 1463–1469]. The one-dimensional concept of multiple augmenting thermodynamic fields by Lesieutre [(1992) *Int. J. Solids Structures* **29**, 1567–1579] is generalized to a suitable three-dimensional continuum form through the introduction of a special type of hidden coordinate vectors with linear, first order, time domain relaxation equations. Consistent with the hidden coordinates, a free energy density function, assuming isothermal conditions, is introduced as the time domain basis of the augmented Hooke's law. Through a time-domain model of the coupled evolution of the mechanical displacements and the thermodynamical variables, issues of causality are avoided completely in the final frequency domain formulation. The general time-domain model used is shown to be equivalent to a three-dimensional, multiple anelastic displacement field model. An isotropic augmented Hooke's law with both dilatational and shearing damping has been implemented and tested using a 20-node volume element in the finite element code ASKA Acoustics. A close agreement between finite element calculations and the corresponding analytically exact results for the studied rod and beam cases is obtained.

NOMENCLATURE

AHL	augmented Hooke's law
a^l_{ik}	affinity, thermodynamic "force" conjugate to thermodynamic variable ε^l_{ik}
A^l	six-dimensional affinity vector conjugate to thermodynamic variable vector E^l
C_{iklm}	elastic moduli in Hooke's generalized law
$\mathbf{D}$	spatial, first order, partial differential operator matrix (6×3 operator matrix)
$\mathbf{D}^T$	spatial, first order, partial differential operator; the 3×6 matrix transpose of $\mathbf{D}$
E	six-dimensional infinitesimal (engineering) strain vector, $E = \mathbf{D}[u]$
E^l	six-dimensional thermodynamic variable vector (hidden coordinate vector)
$\mathbf{F}_l$	coupling 6×6-matrix, between E and E^l, in augmented free energy density
$\mathbf{G}_l$	positive 6×6-matrix in augmented free energy density and entropy production γ
G	elastic shear modulus, Lamé's shear constant (Pa)
$\mathbf{H}$	real, symmetric material modulus 6×6-matrix in Hooke's generalized law (Pa)
$\mathbf{H}_\lambda$	real, symmetric 6×6-matrix in isotropic Hooke's generalized law
$\mathbf{H}_G$	real, diagonal 6×6-matrix in isotropic Hooke's generalized law
$\hat{\mathbf{H}}$	complex, symmetric material modulus 6×6-matrix in augmented Hooke's law
I	time interval $(0, T)$ with length T s
$\mathbf{K}$	real, symmetric (unrelaxed) high-frequency material modulus matrix (6×6)
l	indexing number for thermodynamic processes, variable vectors and parameters
N_a	total number of anelastic, thermodynamic processes (damping processes)
s	complex frequency (Laplace variable) with imaginary part ω (frequency in rad s^{-1})
t	time variable
u	three-dimensional displacement field with Cartesian components $u_i = u_i(\mathbf{x}, t)$
$\mathbf{x}$	point in three-dimensional space with rectangular Cartesian coordinates x_1, x_2, x_3
α, α_l	"dissipation" parameter in isotropic AHL (Pa)
β, β_l	AHL frequency parameter, inverse of relaxation time (rad s^{-1})
γ	local specific entropy production at $\mathbf{x}$ per unit time [$N\,m$(kg^{-1} s^{-1} K^{-1})]
$\bar{\gamma}_I$	mean entropy production at $\mathbf{x}$ per unit mass and unit time during time interval I
ε_{ik}	infinitesimal, symmetric, Cartesian, strain tensor components
ε^l_{ik}	hidden coordinate (or anelastic "strain") in thermodynamic process number l
θ	temperature field in three-dimensional continuum (K)
λ	Lamé's constant (Pa)
μ, μ_l	coupling parameter in isotropic AHL (Pa)

ρ mass density field
σ six-dimensional stress vector corresponding to the engineering strain vector E
σ_{ik} symmetric, Cartesian, stress tensor components (Pa)
φ, φ_l coupling parameter in isotropic AHL (Pa)
ψ specific free energy (N m kg^{-1})
Ψ free energy density function (N m m^{-3})
ω circular frequency corresponding to frequency $f = \omega/2\pi$ in Hz
∇ the three-dimensional, spatial gradient operator
$\dot{u}$ the partial time derivative $\partial u/\partial t$ of u
$\tilde{u}$ the Laplace transform of $u = u(\mathbf{x}, t)$ with respect to the time variable t

1. INTRODUCTION

It is a well known fact that vibration damping caused by dissipation of mechanical energy occurs in all real structures and materials as they vibrate and deform due to external forces and impinging sound waves. Commonly used design materials such as metals and composite materials often, though, have very small damping capacity. In many cases, for example in connection to air, space and surface transportation, this is a problem because effective vibration damping and low sound levels are highly desired design goals.

In built-up structures, such as aircraft, ship and submarine hulls and car bodies, joints and interfaces between structural parts are usually the dominating sources of damping. Even though material damping, i.e. loss of vibration energy due to internal processes inside structural parts, seldom dominates the total system damping there is a real need for accurate material damping modelling techniques. Material damping models, including the spatial distribution and frequency dependence of the damping, are needed as important parts in computation and prediction of, for example, aircraft interior noise caused by acoustic propeller excitation. Yet another example of the same kind is prediction of external noise in the water outside a submarine hull caused by inboard machinery. Generally, material damping cannot be neglected in engineering applications when sound transmission and vibration levels should be predicted or analysed with high accuracy.

There exists a vast amount of literature and results on damping [see for example Ruzicka (1960), Bert (1973), Nashif *et al.* (1985), Kinra and Wolfenden (1992) and references therein] but until recently there have been few methods available that effectively, and in a straightforward manner, account for the frequency dependence and the spatial distribution of material damping in real structures.

A very promising method for dealing with the frequency dependence of material damping was proposed by Lesieutre (1989). His method, which is based on so-called augmenting thermodynamic fields, has since then been discussed by Lesieutre and Mingori (1990) and improved by Lesieutre (1992) and Lesieutre and Bianchini (1993). Lesieutre (1989–1992) and Lesieutre and Mingori (1990) treat one-dimensional cases only, while a three-dimensional formulation based on anelastic displacement fields is presented in Lesieutre and Bianchini (1993). In several aspects Lesieutre's method is new, at least in the field of structural dynamics and vibroacoustics.

In addition to Lesieutre's work, considerable progress in modelling viscoelastic material behavior has been reported, as presented, in the works by Bagley and Torvik (1983) on *fractional derivative models*, Golla and Hughes (1985) and McTavish and Hughes (1993) on *mini-oscillator models* and by Yiu (1993) on *generalized Maxwell models*. The mini-oscillator model, the generalized Maxwell model as well as Lesieutre's model are all based on the concept of internal dissipation coordinates. They all result in expanded and larger time domain finite element mass, stiffness and damping matrices and more degrees of freedom when compared to corresponding elastic finite element models. Both fractional derivative models and mini-oscillator models are reported to fit experimental data over broad ranges of frequency (Bagley and Torvik 1983; McTavish and Hughes, (1993).

Differences and similarities between the augmented Hooke's law (AHL) approach, which is proposed here, and *anelastic displacement models*, *fractional derivative models* and *mini-oscillator models* for damping simulation will be addressed by the author in a forthcoming paper. The AHL method and classical viscoelasticity and similarities with Yiu's work on viscoelastic structures, (Yiu, 1993), will also be discussed in a separate paper.

In the present paper, a fully three-dimensional material damping modelling technique is proposed. The method is formulated in the frequency domain as an augmented Hooke's law, in which material damping is introduced by adding frequency dependent, complex anelastic terms to the material modulus matrix of Hooke's generalized law.

Important advantages of the AHL formulation are that:

it can be directly implemented, as a complex valued constitutive matrix, in any finite element code incorporating complex node variables, complex element (material) properties and a complex equation solver,

spatial (i.e. element) and frequency dependent damping, can be introduced in finite element models in a natural way without need for extra degrees of causality freedom, problems, in the damping description, are avoided completely because the basic assumptions are formulated in the time domain, even though the resulting AHL formulation is a frequency domain method.

The derivations leading to the augmented Hooke's law are inspired by Lesieutre's results, (Lesieutre, 1989, 1992a, 1992b), and his basic assumptions concerning augmenting thermodynamic fields and their corresponding first order, linear equations of evolution (Section 3). It should be noted that the augmenting thermodynamic fields are analogous to hidden coordinates of the same kind as those introduced by Biot (1954, 1955, 1956, 1958, 1959) in his linear theory of irreversible thermodynamics. It should also be noted that there exists a formal resemblance between the augmented Hooke's law and Biot's operational equation results (Biot, 1955). The concept of hidden coordinates, also called internal variables in the literature, and Biot's linear theory of irreversible thermodynamics is taken here as the theoretical basis of the AHL formulation and the linear augmented Hooke's law.

The originality of the present paper is:

(a) *generalization* of Lesieutre's basic one-dimensional assumptions to a suitable three-dimensional form by introduction of a special type of anelastic strains as hidden coordinates (Section 3.1),

(b) *formulation* of a new free energy density function for isothermal conditions (Section 3.2),

(c) *derivation* of the resulting augmented Hooke's law, AHL, based on (a) and (b) above (Section 4) and

(d) *derivation* of the entropy production associated with the augmented Hooke's law, based on (a)–(c) above and the Clausius–Duhem inequality (Section 5).

The isotropic AHL formulation, presented in Section 6, has been implemented (Section 7.1) in the finite element code ASKA Acoustics (Göransson, 1988), as a complex, frequency dependent, fully three-dimensional, symmetric and isotropic element. Numerical tests and comparisons to one-dimensional analytical solutions have been done with quite satisfactory results (Sections 7.2 and 7.3).

2. THE ELASTIC, GENERALIZED HOOKE'S LAW

Throughout the discussions to follow a three-dimensional continuum with displacements u_i and stresses σ_{ik} is considered. When the body forces vanish the equations of motion of the continuum, expressed in rectangular Cartesian coordinates x_1, x_2, x_3 are (Fung, 1965):

$$-\frac{\partial \sigma_{ik}}{\partial x_k} + \rho \ddot{u}_i = 0 \quad i = 1, 2, 3. \tag{1}$$

For a linear, purely elastic material the stresses under isothermal conditions are:

$$\sigma_{ik} = \mathrm{C}_{iklm}\varepsilon_{lm}, \tag{2}$$

where C_{iklm} are elastic constants or moduli which generally are functions of the spatial coordinates. The functions ε_{ik} are the Cartesian components of the infinitesimal strain tensor and the summation convention is implied in both eqns (1) and (2).

Equations (2) constitute Hooke's generalized law which conveniently is expressed in standard engineering matrix notation as:

$$\sigma = \mathbf{H}E, \tag{3}$$

where E is the six-dimensional infinitesimal (engineering) strain vector:

$$E = \mathbf{D}[u]. \tag{4}$$

The vector σ is the corresponding six-dimensional stress vector while $\mathbf{H}$ is the real, symmetric, positive material modulus matrix. Details about the 6×6 matrix $\mathbf{H}$ may be found in, for example, Reddy (1986). Cartesian stress and strain tensor components and matrix notation as above will be used throughout the paper. The (matrix) column vector fields σ, E and u and the first order spatial, partial differential (matrix) operator $\mathbf{D}$ are defined in the Appendix.

Using internal, thermodynamic variables and a new free energy density as a basis it will be shown in the following that material damping, including the spatial as well as the frequency dependence, can be accounted for in the frequency domain by adding complex valued, frequency dependent, symmetric terms to the real, symmetric and frequency independent Hooke's law matrix $\mathbf{H}$.

3. ANELASTICITY ASSUMPTIONS

3.1. *Internal variables*

The basic assumption made by Lesieutre for an "augmenting thermodynamic field", ξ, is the scalar equation of evolution or the relaxation equation:

$$\dot{\xi} = -\beta(\xi-\xi_0), \tag{5}$$

where ξ_0 is the *strain dependent thermodynamic equilibrium value* of ξ and β is a positive material constant defined as the inverse of a *finite* relaxation time constant. The fundamental idea behind the thermodynamic variable ξ is that its interaction with the mechanical displacements in the continuum is associated with entropy production and, thus, with material damping. The physical relevance behind these ideas will not be discussed in the present paper but they will be used as a starting point for the AHL formulation. For a detailed discussion of thermodynamic variables, hidden coordinates and relaxation equations see Biot (1954, 1955, 1956, 1958), de Groot and Mazur (1962), Fung (1965) and Nowick and Berry (1972).

Assuming that there are N_a different augmenting thermodynamic fields, ξ^l, representing separate damping "mechanisms", the corresponding evolution equations suggested by eqn (5) will be defined by the equations:

$$\dot{\xi}^l = -\beta_l(\xi^l-\xi^l_0) \quad l = 1,2,3,\ldots,N_a; \quad \beta_l > 0 \tag{6}$$

which correspond to a special case of Biot's "basic relations for irreversible processes" (Biot, 1955). Uncoupled relaxation equations of this kind are used by Lesieutre (1992) in his one-dimensional theory of multiple augmenting fields.

Here a slightly different approach is used which is crucial for applications to a three-dimensional continuum. The crucial step is the introduction of a number of six-dimensional vector fields E^l with components defined by symmetric tensor components ε^l_{ik} as:

$$E^l \equiv [\varepsilon_{11}^l \quad \varepsilon_{22}^l \quad \varepsilon_{33}^l \quad 2\varepsilon_{12}^l \quad 2\varepsilon_{23}^l \quad 2\varepsilon_{31}^l]^{\mathrm{T}} \quad l = 1, 2, 3, \ldots, N_{\mathrm{a}}. \tag{7}$$

Through a formal reformulation of eqn (6), based on the assumption that the thermodynamic variables ξ^l are two times continuously differentiable with respect to the spatial coordinates and that the vectors E^l are identified with the fields $\mathbf{D}[\nabla\xi^l]$, the thermodynamic vector fields E^l may be assumed to have the first order linear evolution equations:

$$\dot{E}^l + \beta_l E^l = \beta_l E_0^l \quad l = 1, 2, 3, \ldots, N_{\mathrm{a}}; \tag{8}$$

where the parameters β_l are positive. The thermodynamical equilibrium values E_0^l in eqn (8) will later be shown to be linear functions of the current mechanical strain represented by the vector field E. From now on the vector fields E^l, interchangeably with the corresponding tensor components ε_{ik}^l, will be denoted anelastic strains and used as hidden coordinate vectors with matrix evolution equations (8).

Note that the requirement of causality, in the damped, three-dimensional continuum description is accounted for automatically, because the basic anelasticity assumptions (7) and (8) are formulated in the time domain. This is an advantage of the AHL formulation, shared also by Lesieutre's one- and three-dimensional formulations, as compared to other commonly used models (Bert, 1973) of material damping.

Stresses, affinities and thermodynamical equilibrium vector fields E_0^l can be defined only after a suitable free energy density function has been introduced.

3.2. *Free energy assumption*

Define the *free energy density* Ψ per unit volume at *isothermal conditions* as:

$$\Psi \equiv \rho\psi \equiv \tfrac{1}{2}E^{\mathrm{T}}\mathbf{K}E - \sum_{l=1}^{N_{\mathrm{a}}} E^{\mathrm{T}}\mathbf{F}_l E^l + \sum_{l=1}^{N_{\mathrm{a}}} \tfrac{1}{2}E^{l\mathrm{T}}\mathbf{G}_l E^l \tag{9}$$

$$\mathbf{K} \equiv \mathbf{H} + \sum_{l=1}^{N_{\mathrm{a}}} \mathbf{F}_l \mathbf{G}_l^{-1} \mathbf{F}_l \tag{10}$$

[cf. Lesieutre (1989)] where ψ is the *specific free energy* (the free energy per unit mass). The matrices $\mathbf{G}_l$ must be real, symmetric and positive while the matrices $\mathbf{F}_l$ must be real and symmetric. The required symmetry of the matrices is a consequence of the symmetry of the current stress and strain tensors and the symmetry of the anelastic strain tensors ε_{ik}^l. The positiveness, of $\mathbf{H}$ and the matrices $\mathbf{G}_l$, follows from the requirement that the free energy must be positive in the neighbourhood of the natural state (Fung, 1965), of the continuum. The physical dimension and units of the matrices $\mathbf{F}_l$ and $\mathbf{G}_l$ are the same as those of the elastic moduli in the Hooke's matrix $\mathbf{H}$ when the hidden coordinates ε_{ik}^l are assumed to be dimensionless.

3.3. *Time domain evolution equations*

To proceed with the formulation of the augmented Hooke's law, the stresses σ_{ik} are defined as:

$$\sigma_{ik} \equiv \frac{\partial\Psi}{\partial\varepsilon_{ik}} \tag{11}$$

and the six-dimensional stress vector field σ is correspondingly expressed as:

$$\sigma = \mathbf{K}E - \sum_{l=1}^{N_{\mathrm{a}}} \mathbf{F}_l E^l \tag{12}$$

which according to eqn (10) may also be written:

$$\sigma = \mathbf{H}E + \sum_{l=1}^{N_a} \mathbf{F}_l \mathbf{G}_l^{-1}[\mathbf{F}_l E - \mathbf{G}_l E^l]. \tag{13}$$

The affinities or "thermodynamic forces" a_{ik}^l corresponding to the anelastic strains ε_{ik}^l are given by:

$$a_{ik}^l \equiv -\frac{\partial \Psi}{\partial \varepsilon_{ik}^l} \tag{14}$$

and the corresponding six-dimensional affinity vector A^l as:

$$A^l = \mathbf{F}_l E - \mathbf{G}_l E^l. \tag{15}$$

The thermodynamic, anelastic equilibrium strains E_0^l in eqn (8) may now, according to eqn (15), be determined as the anelastic strains corresponding to zero affinities A^l, i.e. as:

$$E_0^l \equiv E^l|_{a_{ik}^l = 0} = \mathbf{G}_l^{-1} \mathbf{F}_l E. \tag{16}$$

From a substitution of (15) into (13) and of (16) into (15) it follows that:

$$\sigma = \mathbf{H}E + \sum_{l=1}^{N_a} \mathbf{F}_l \mathbf{G}_l^{-1} A^l \tag{17}$$

$$A^l = -\mathbf{G}_l[E^l - E_0^l]. \tag{18}$$

It is obvious from eqn (17) that the current stress vector, σ, is obtained by adding anelastic terms to the "elastic" part $\mathbf{H}E$. According to eqns (17), (18) and (8) the stress becomes elastic and obeys Hooke's generalized law (3), when the thermodynamic forces A^l or, equivalently, the anelastic strain velocities $\dot{E}^l$ all vanish. Details about affinities and linear evolution equations may be found in de Groot and Mazur (1962) and Nowick and Berry (1972).

When the stresses (12) are substituted into the equations of motion (1) the resulting matrix equation is (see Appendix for the definition of the first order spatial, partial differential (matrix) operators $\mathbf{D}$ and $\mathbf{D}^T$):

$$-\mathbf{D}^{\mathrm{T}}[\mathbf{K}\mathbf{D}[u]] + \rho \ddot{u} = -\sum_{l=1}^{N_a} \mathbf{D}^{\mathrm{T}}[\mathbf{F}_l E^l] \tag{19}$$

which is a coupled partial differential equation for the three-dimensional displacement field $u = u(\mathbf{x}, t)$ and the anelastic strain fields $E^l = E^l(\mathbf{x}, t)$.

To conclude the discussion of anelasticity, (16) may be substituted into (8) and the final evolution equations for the anelastic strains are obtained as:

$$\dot{E}^l + \beta_l E^l = \beta_l \mathbf{G}_l^{-1} \mathbf{F}_l \mathbf{D}[u] \quad l = 1, 2, 3, \ldots, N_a; \quad \beta_l > 0 \tag{20}$$

which are the fundamental thermodynamic, time domain evolution equations governing the AHL formulation and the augmented Hooke's law.

The equations (19) and (20) together, in Cartesian matrix notation, govern the evolution and motion of the studied three-dimensional continuum. The question of boundary conditions, which the mechanical displacements u_i and the stresses σ_{ik} must satisfy, are mentioned in Section 4.

3.4. *Comment on anelastic displacement fields*

Assuming that six-dimensional vector fields E_a^l, corresponding to three-dimensional anelastic displacement fields u_a^l, are identified as the transformed anelastic strains:

$$E_a^l \equiv \mathbf{D}[u_a^l] \equiv \mathbf{K}^{-1}\mathbf{F}_l E^l \quad l = 1, 2, 3, \ldots, N_a \tag{21}$$

it follows that the AHL evolution equations (20) are equivalent to the evolution equations:

$$\dot{E}_a^l + \beta_l E_a^l = \beta_l \mathbf{K}^{-1}\mathbf{F}_l \mathbf{G}_l^{-1}\mathbf{F}_l E \quad l = 1, 2, 3, \ldots, N_a; \quad \beta_l > 0 \tag{22}$$

for the transformed strains E_a^l. It also follows that the stress vector σ is given by:

$$\sigma = \mathbf{K}(E - \mathbf{D}[u_a]) \tag{23}$$

where the total anelastic displacement field u_a is defined as the sum:

$$u_a \equiv \sum_{l=1}^{N_a} u_a^l. \tag{24}$$

Using the anelastic displacement fields, formally defined by eqns (21) and (24), the evolution equations (22) and the free energy (9) as a starting point it may be possible to derive a time domain model analogous to the three-dimensional, multiple anelastic displacement model presented by Lesieutre and Bianchini (1993).

4. AUGMENTED HOOKE'S LAW IN FREQUENCY DOMAIN

4.1. *Constitutive equations*

In the following the Laplace transform of a field or function is denoted by a tilde above the particular parameter, i.e. if p is the time domain variable then $\tilde{p}$ denotes the Laplace transform of p. By application of the Laplace transform to the equations (12) and (20) above the augmented Hooke's law may be derived through elimination of the transformed anelastic strains $\tilde{E}^l$.

Laplace transformation of eqns (12) and (20), assuming zero initial conditions for the anelastic strain vectors E^l, will result in the equations:

$$\tilde{\sigma} = \mathbf{K}\tilde{E} - \sum_{l=1}^{N_a} \mathbf{F}_l \tilde{E}^l \tag{25}$$

$$(s + \beta_l)\tilde{E}^l = \beta_l \mathbf{G}_l^{-1}\mathbf{F}_l \mathbf{D}[\tilde{u}], \quad l = 1, 2, 3, \ldots, N_a; \quad \beta_l > 0 \tag{26}$$

where s is the complex Laplace or frequency variable with a circular frequency imaginary part ω.

Substitution of (4) in (26) and elimination of $\tilde{E}^l$ between (25) and (26), results in:

$$\tilde{\sigma} = \hat{\mathbf{H}}\tilde{E}, \tag{27}$$

where $\hat{\mathbf{H}} = \hat{\mathbf{H}}(\mathbf{x}, s)$ is the complex valued, frequency dependent constitutive 6×6 matrix:

$$\hat{\mathbf{H}} = \mathbf{H} + \sum_{l=1}^{N_a} \frac{s}{(s + \beta_l)} \mathbf{F}_l \mathbf{G}_l^{-1}\mathbf{F}_l \tag{28}$$

or equivalently:

$$\hat{\mathbf{H}} = \mathbf{K} - \sum_{l=1}^{N_a} \frac{\beta_l}{(s+\beta_l)} \mathbf{F}_l \mathbf{G}_l^{-1} \mathbf{F}_l. \tag{29}$$

Equations (27)–(29) with frequency dependent constitutive, complex valued material modulus matrix $\hat{\mathbf{H}}$ constitutes the *augmented Hooke's law* in frequency domain for a fully three-dimensional and anisotropic material. It is obvious, from eqn (28), that the AHL matrix at zero frequency equals **H**. Thus will the augmented Hooke's law approach the usual generalized Hooke's law for low frequency vibrations and generally slow processes. At high frequencies $\hat{\mathbf{H}}$, according to eqn (29), approaches the unrelaxed, high frequency material modulus matrix **K**, as expected.

At this point it should be noted that a more complicated frequency dependence in each added term in eqn (28) may be simulated. As an example, this may be achieved by grouping damping mechanisms with proportional $\mathbf{F}_l \mathbf{G}_l^{-1} \mathbf{F}_l$-matrices together in the sum in eqn (28), i.e. by using contributions of the type, cf. Lesieutre (1992):

$$\left[\sum_{l=N}^{M} \frac{s \cdot a_l}{(s+\beta_l)} \right] \mathbf{F} \mathbf{G}^{-1} \mathbf{F} \tag{30}$$

with real coefficients a_l.

It should also be noted that the derivation of the augmented Hooke's law equally well could have been based on anelastic displacements u_a^l as defined in eqns (21) and (24) above. Thus, formally, the AHL approach is analogous to a frequency domain version of the three-dimensional, multiple, anelastic displacement model presented by Lesieutre and Bianchini (1993). Advantages of the AHL approach, over Lesieutre's time domain method, are that it does not introduce any extra degrees of freedom into the final frequency domain equations of motion and that the corresponding finite element equations contain symmetric matrices only. A restriction of the AHL method, though, is that it is completely linear and thus cannot handle non-linear, temperature dependent high dissipation damping problems such as "thermal runaway" discussed by Lesieutre and Govindswamy (1994).

4.2. *Equations of motion*

Assuming zero initial conditions for the displacement field $u = u(\mathbf{x}, t)$ and the corresponding velocity field $\dot{u} = \dot{u}(\mathbf{x}, t) \equiv (\partial u/\partial t)$, Laplace transformation of the equations of motion (1) yields the matrix equation:

$$-\mathbf{D}^{\mathrm{T}}[\tilde{\sigma}] + s^2 \rho \tilde{u} = \mathbf{0}. \tag{31}$$

When stresses, defined according to the augmented Hooke's law (27), are introduced into this equation the resulting frequency domain, partial differential equation for the transformed displacement field $\tilde{u} = \tilde{u}(\mathbf{x}, s)$ is obtained as:

$$-\mathbf{D}^{\mathrm{T}}[\hat{\mathbf{H}}\mathbf{D}[\tilde{u}]] + s^2 \rho \tilde{u} = \mathbf{0}. \tag{32}$$

The transformed displacement field $\tilde{u} = \tilde{u}(\mathbf{x}, s)$ and the transformed traction field $\tilde{t}_{\mathbf{n}} = \tilde{t}_{\mathbf{n}}(\mathbf{x}, s)$ also have to satisfy appropriate transformed boundary conditions (essential, natural or mixed) on the boundary of the studied continuum. In this context it should be noted that the anelastic (time domain) hidden coordinates introduced in Section 3 do not appear explicitly in the augmented Hooke's law (27)–(29), nor in the frequency domain partial differential equation (32) or in the corresponding frequency domain boundary conditions. As a result, eqn (32), together with its frequency domain boundary conditions, under isothermal conditions governs the motion of a three-dimensional continuum with AHL material properties.

5. ENTROPY PRODUCTION

Expressions derived, which define the entropy production locally in different parts of a vibrating structure, may be of considerable practical interest in applications when the effect of different kinds and placements of damping treatments are studied. It should, e.g. when computing and predicting vibrational response, be possible to identify parts where most of the energy dissipation will take place during a specific vibrational excitation.

A suitable starting point for derivation of the (local) entropy production due to damping is the Clausius–Duhem inequality, as presented by Truesdell and Noll (1992), which states that the entropy production is always non-negative. Under isothermal conditions, it follows from eqns (9), (12) and (15) that the local entropy production γ per unit mass and unit time for a material obeying the augmented Hooke's law (27) is given by:

$$\rho\gamma = \frac{1}{\theta}\sum_{l=1}^{N_a} A^{l\mathrm{T}}\dot{E}^l. \tag{33}$$

Combining (33) with (18) and the evolution equations (8) and recalling that all the β_l and $\mathbf{G}_l$ are positive, it is easily shown that each anelastic strain velocity vector $\dot{E}^l$ is associated with a non-negative entropy production γ_l:

$$\rho\gamma_l \equiv \frac{1}{\theta}\cdot\frac{1}{\beta_l}\dot{E}^{l\mathrm{T}}\mathbf{G}_l\dot{E}^l \geqslant 0 \tag{34}$$

per unit mass and unit time. The entropy production corresponding to the augmented Hooke's law thus is non-negative and in agreement with the Clausius–Duhem inequality.

For a time harmonic (sinusoidal) strain field $E = E(\mathbf{x}, t)$:

$$E = \mathrm{Re}\,[C(\mathbf{x})\cdot \mathrm{e}^{\mathrm{i}\omega t}] \tag{35}$$

corresponding to a steady state time harmonic vibration with angular frequency ω, it may be shown that the mean value $\bar{\gamma}_l$ of the entropy production, at point $\mathbf{x}$ during a time interval $I \equiv (0, T)$ is given by:

$$\bar{\gamma}_l(\mathbf{x}) = \frac{1}{8}\cdot\frac{1}{\rho\theta}\sum_{l=1}^{N_a}\frac{\beta_l\cdot\omega^2}{(\beta_l^2+\omega^2)}\mathbf{C}^{\mathrm{T}}\mathbf{F}_l\mathbf{G}_l^{-1}\mathbf{F}_l C^*. \tag{36}$$

The $\mathbf{x}$-dependent, complex valued strain "amplitude" vector $C = C(\mathbf{x})$, with complex conjugate C^*, is defined by the strain vector field E as:

$$C \equiv \frac{2}{\mathrm{T}}\cdot\int_0^T \mathrm{e}^{-\mathrm{i}\omega t}E(\mathbf{x}, t)\,\mathrm{d}t. \tag{37}$$

If the complex valued vector $C(\mathbf{x})$ corresponds to, e.g., a computed response due to a known time harmonic excitation of the continuum, then the spatial distribution of the mean entropy production per unit mass and unit time may be computed according to the expression (36).

6. ISOTROPIC AUGMENTED HOOKE'S LAW

6.1. *Constitutive equation*

For isotropic, elastic materials the generalized Hooke's law matrix **H** may be written:

$$\mathbf{H} = \lambda \cdot \mathbf{H}_\lambda + G \cdot \mathbf{H}_G, \tag{38}$$

where λ and G are the usual real Lamé's constants. The only *non-zero elements* of the constant, real and symmetric matrices $\mathbf{H}_\lambda$ and $\mathbf{H}_G$ are:

$$(\mathbf{H}_\lambda)_{ik} = 1 \quad i,k \leqslant 3 \tag{39}$$

$$(\mathbf{H}_G)_{ii} = 2 \quad 1 \leqslant i \leqslant 3$$

$$(\mathbf{H}_G)_{ii} = 1 \quad 4 \leqslant i \leqslant 6. \tag{40}$$

An isotropic AHL material with anelastic strain vectors E^l, representing physically different "damping mechanisms", will now be defined using the general results in Sections 3 and 4. According to the eqns (17), (18) and (8) the time domain stress vector may be expressed as:

$$\sigma = \mathbf{H}E + \sum_{l=1}^{N_a} \frac{1}{\beta_l} \mathbf{F}_l \dot{E}^l \tag{41}$$

with positive frequency parameters β_l and an isotropic AHL is obtained by assuming that each coupling matrix $\mathbf{F}_l$ in the sum is a linear combination of the matrices $\mathbf{H}_\lambda$ and $\mathbf{H}_G$, (39) and (40):

$$\mathbf{F}_l = \varphi_l \cdot \mathbf{H}_\lambda + \mu_l \cdot \mathbf{H}_G. \quad l = 1, 2, 3, \ldots, N_a. \tag{42}$$

In eqns (41) and (42) each of the parameters β_l, φ_l and μ_l are supposed to be real material parameters which are in general **x**-dependent.

The $\mathbf{G}_l$-matrices in the free energy density Ψ, cf. (9) and (10), also have to be defined. A possible assumption here is to choose the $\mathbf{G}_l$-matrices as diagonal and, e.g.,

$$(\mathbf{G}_l)_{ik} = \begin{cases} \alpha_l \cdot \delta_{ik}, & 1 \leqslant i,k \leqslant 3 \\ \dfrac{\alpha_l}{2} \cdot \delta_{ik}, & 4 \leqslant i,k \leqslant 6 \end{cases}, \tag{43}$$

where each α_l is positive and δ_{ik} is the Kronecker delta.

When the assumptions (42) and (43) are introduced it is obtained that:

$$\mathbf{F}_l \mathbf{G}_l^{-1} \mathbf{F}_l = \frac{(3\varphi_l^2 + 4\varphi_l \mu_l)}{\alpha_l} \cdot \mathbf{H}_\lambda + \frac{2\mu_l^2}{\alpha_l} \cdot \mathbf{H}_G \tag{44}$$

and thus, according to eqn (28), the *isotropic augmented Hooke's law matrix* finally equals:

$$\hat{\mathbf{H}} = \mathbf{H} + \sum_{l=1}^{N_a} \frac{s}{(s+\beta_l)\alpha_l} [(3\varphi_l^2 + 4\varphi_l \mu_l) \cdot \mathbf{H}_\lambda + 2\mu_l^2 \cdot \mathbf{H}_G]. \tag{45}$$

According to eqn (38) this isotropic, augmented Hooke's law also may be written:

$$\hat{\mathbf{H}} = \left[\lambda + \sum_{l=1}^{N_a} \frac{s \cdot a_l}{(s+\beta_l)}\right]\mathbf{H}_\lambda + \left[G + \sum_{l=1}^{N_a} \frac{s \cdot b_l}{(s+\beta_l)}\right]\mathbf{H}_G, \tag{46}$$

where the parameters a_l and b_l are:

$$a_l \equiv \frac{3 \cdot \varphi_l^2 + 4\varphi_l \mu_l}{\alpha_l} \quad l = 1, 2, \ldots, N_a \tag{47}$$

$$b_l \equiv \frac{2 \cdot \mu_l^2}{\alpha_l}, \quad l = 1, 2, \ldots, N_a. \tag{48}$$

Thus, each separate "damping mechanism", identified with subscript l, is characterized by four parameters α_l, β_l, φ_l and μ_l.

6.2. *General remarks*

It should be noted that, with the constitutive equation adopted here, a mixed normal strain and shear strain damping model is obtained for processes with μ_l different from zero. This will be the case even if the corresponding parameter φ_l equals zero. The mixed nature of the anelastic stress contributions becomes more clear when the anelastic parts of, e.g., the stresses $\tilde{\sigma}_{11}$ and $\tilde{\sigma}_{12}$ corresponding to eqn (46) are written out in detail, respectively, as:

$$(\tilde{\sigma}_{11})_a = \frac{s \cdot (3\varphi_l^2 + 4\varphi_l \mu_l)}{(s+\beta_l)\alpha_l}(\tilde{\varepsilon}_{11} + \tilde{\varepsilon}_{22} + \tilde{\varepsilon}_{33}) + \frac{s \cdot 4\mu_l^2}{(s+\beta_l)\alpha_l}\tilde{\varepsilon}_{11}$$

$$(\tilde{\sigma}_{12})_a = \frac{s \cdot 2\mu_l^2}{(s+\beta_l)\alpha_l} \cdot 2\tilde{\varepsilon}_{12}.$$

It is obvious from these expressions that the φ_l-contribution to the damping may not be isolated from the μ_l-contribution and studied separately. On the contrary, the μ_l-contribution may be studied separately under pure shear deformation.

It may also be noted, following from eqns (46)–(48), that *proportional damping*, Ewins (1986), will be obtained in an isotropic AHL material if the condition:

$$\frac{3\varphi_l^2 + 4\varphi_l \mu_l}{2\mu_l^2} = \frac{\lambda}{G} \tag{49}$$

is fulfilled for all $l = 1, 2, \ldots, N_a$ at all points $\mathbf{x}$ in the material. It follows from eqns (38) and (46) that the AHL matrix $\hat{\mathbf{H}}$, in this case, would be *proportional to the Hooke's law matrix* $\mathbf{H}$ with a complex, frequency dependent proportionality factor.

The augmented Hooke's law defined by eqns (46)–(48) may be viewed as a generalization to three dimensions and isotropic AHL materials of the one-dimensional case with "multiple augmenting fields" presented by Lesieutre (1992). Multiple processes and isotropic materials are also discussed by Lesieutre and Bianchini (1993) but a comparison with their work will not be done here (cf. Section 1).

7. THREE-DIMENSIONAL FINITE ELEMENT IMPLEMENTATION

7.1. *Volume element implementation*

The isotropic augmented Hooke's law, defined by eqns (46)–(48), has been implemented in the ASKA Acoustics code (Göransson 1988) as a complex valued, frequency dependent 20-node volume element called HXAHL20.

Three different *isotropic, single process damping* cases may currently be chosen for this element:

- $\varphi \neq 0 \quad \mu = 0 \qquad$ -φ-damping
- $\varphi = 0 \quad \mu \neq 0 \qquad$ -μ-damping
- $\varphi \neq 0 \quad \mu \neq 0. \qquad$ -$\varphi\mu$-damping

The damping parameters α, β, φ and μ are constant throughout the element.

7.2. *Application to a one-dimensional rod*

It may be shown that an analytical solution for a one-dimensional rod with a single AHL damping mechanism involves a rod with frequency dependent, complex valued material modulus $m(s)$:

$$m(s) = E_Y + \frac{s}{(s+\beta)} \cdot \frac{\delta^2}{\alpha}, \quad \alpha, \beta > 0 \tag{50}$$

where the positive factor δ^2/α corresponds to a matrix product $\mathbf{F}_l \mathbf{G}_l^{-1} \mathbf{F}_l$ in the general three dimensional expression for $\hat{\mathbf{H}}$ in eqn (28). The parameters β (the inverse of a relaxation time constant), δ (the strength of coupling between the thermodynamical variable and the current strain) and α are the same as used by Lesieutre (1989, 1992a) and E_Y is the Young's modulus.

The complex valued displacement amplitude $u(L)$ at $x = L$ and circular frequency ω, for a rod with complex modulus (50), is given by:

$$u(L) = \frac{F\kappa}{\rho A \omega^2} \tan(\kappa L), \tag{51}$$

where κ is the complex, frequency dependent wave number defined by:

$$\kappa^2 \equiv \frac{\rho\omega^2}{m(\mathrm{i}\omega)} = \frac{\rho\omega^2(\beta + \mathrm{i}\omega)}{E_Y\left[\beta + \mathrm{i}\omega\left(1 + \dfrac{\delta^2}{E_Y \alpha}\right)\right]}. \tag{52}$$

In this case the rod is assumed to vibrate longitudinally along the x-axis while fixed at $x = 0$. It is excited at the end $x = L$, in the x-direction, by a time harmonic force with amplitude F and circular frequency ω.

For a case with $u_2 = u_3 \equiv 0$, with displacements in the x_1-direction only (the x coordinate is identified with the coordinate x_1), and thus also $\varepsilon_{22} = \varepsilon_{33} \equiv 0$, the isotropic three-dimensional augmented Hooke's law, with a single damping process ($N_a = 1$) is reduced to, see eqns (27) and (46),:

$$\tilde{\sigma}_{11} = \left[\lambda + 2G + \frac{s \cdot (3\varphi^2 + 4\varphi\mu)}{(s+\beta)\alpha} + \frac{s \cdot 4\mu^2}{(s+\beta)\alpha}\right]\tilde{\varepsilon}_{11} \tag{53}$$

which is equivalent to:

$$\frac{\tilde{\sigma}_{11}}{\tilde{\varepsilon}_{11}} = \frac{E_Y(1-\nu)}{(1+\nu)(1-2\nu)} + \frac{s}{(s+\beta)} \frac{(\sqrt{3\varphi^2 + 4\varphi\mu})^2}{\alpha} + \frac{s}{(s+\beta)} \frac{(2\mu)^2}{\alpha} \tag{54}$$

where ν is the Poisson's ratio.

It then follows, from eqns (50) and (54), that modified values:

$$E' \equiv \frac{E_Y(1-\nu)}{(1+\nu)(1-2\nu)} \tag{55}$$

$$\delta' \equiv \sqrt{3}\cdot\varphi \tag{56}$$

should be substituted for E_Y and δ in the analytical solution (51), when comparing it to a finite element simulation of the rod with three-dimensional elements, constraints $u_2 = u_3 \equiv 0$ and normal strain damping with damping parameter $\mu = 0$.

The end-displacement (51) has been computed for a rod with cross-section $A = 1\times 1$ m^2, length $L = 10$ m and force amplitude $F = 1$ N. The material parameters chosen were $E_Y = 7.13\cdot 10^{10}\ \text{N m}^{-2}$, $\nu = 0.3$ and $\rho = 2750\ \text{kg m}^{-3}$ and the AHL damping parameters δ, β, α the same as quoted by Lesieutre for aluminium, i.e. $\delta = \varphi = 4.77\cdot 10^6\ \text{N m}^{-2}$, $\beta = 8000$ rad s^{-1} and $\alpha = 8000\ \text{N m}^{-2}$ (Lesieutre, 1989: p. 48). The solid line in Fig. 1 shows the analytical end-displacement $u(L)$ computed according to eqns (51) and (52), with E_Y and δ substituted by E' and δ' in eqns (55) and (56). The dashed line in Fig. 1 shows the same end-displacement calculated for a coupling parameter δ' which is a factor of two larger than for the solid line, i.e. corresponding to four times larger damping. The peaks, for the case with the larger damping, are lowered by a factor of four and displaced to higher frequencies. The frequency shift to higher frequencies is a consequence of the positiveness of the real part of the anelastic term in the one-dimensional augmented Hooke's law (50). As expected, it can also be seen that the amplitude (magnitude) curve approaches the static elastic value $FL/E'A$ at zero frequency.

The rod ($L = 10$ m, $A = 1\times 1\ \text{m}^2$) has been simulated by a three-dimensional finite element model with $20\times 5\times 5$ complex AHL-elements (20 elements in the longitudinal x_1-direction and 5 elements in each transverse direction) and constrained transverse displacements $u_2 = u_3 \equiv 0$ in ASKA Acoustics (Section 7). Geometry, material parameters, AHL damping parameters (α, β, $\varphi = \delta$ and $\mu = 0$) and excitation were chosen as for the analytical rod. The end-displacement computed with ASKA Acoustics is shown in Fig. 2 (solid line). As can be seen, the agreement between the finite element calculation and the

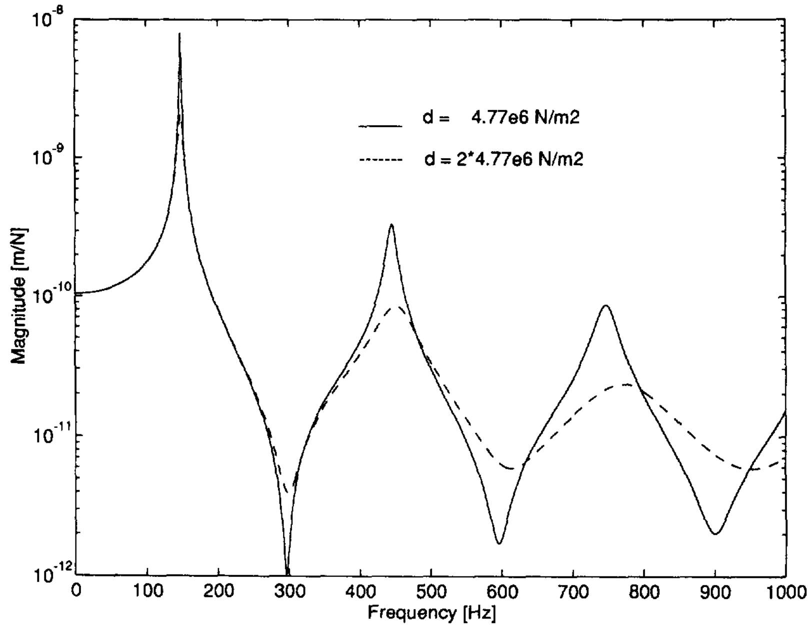

Fig. 1. End-displacement (receptance) of a longitudinally vibrating cantilever rod excited in the axial x-direction by a time harmonic unit force at the free end. Analytical solution with coupling factor $\delta = 4.7766\cdot 10^6$ (solid line) and 2δ (dashed line).

analytical solution (solid line in Fig. 1 and circles in Fig. 2) is excellent in this simple example.

For the rod, vibrating with angular frequency ω and thus having a time harmonic (sinusoidal) strain field $\varepsilon = \partial u/\partial x = \mathrm{Re}\,[c(x)\,\mathrm{e}^{i\omega t}]$, it may be shown [cf. eqns (35)–(37)] that the (local) *mean entropy production* $\bar{\gamma}_I$ per unit mass and unit time at point x and temperature θ, during a time interval $I = (0, T)$, is given by:

$$\rho\theta\cdot\bar{\gamma}_I = \tfrac{1}{8}\cdot|c|^2\cdot\frac{\beta\delta^2}{\alpha}\cdot\frac{\omega^2}{(\beta^2+\omega^2)}, \tag{57}$$

where $|c| = |c(x)|$ is the (real) strain amplitude at point x. It follows from eqn (57) that the entropy production is bounded by:

$$\rho\theta\cdot\bar{\gamma}_I \to \frac{|c|^2}{8}\cdot\beta\cdot\frac{\delta^2}{\alpha} \quad \text{when} \quad \omega\to\infty. \tag{58}$$

It should be noted that the parameter δ^2/α corresponds to a matrix product $\mathbf{F}_I\mathbf{G}_I^{-1}\mathbf{F}_I$ in the general three-dimensional case [cf. eqn (36)].

7.3. *Three-dimensional test examples*

The finite element model used for the simulation of the one-dimensional cantilever rod, discussed in Section 8, has also been used to simulate an *isotropic three-dimensional cantilever beam* in "plane" bending and mixed bending and torsion. The *bending* vibration (case B) was excited by a symmetrically and uniformly distributed, time harmonic transverse force $F = 1$ N in the x_2-direction at the free end $x = x_1 = L = 10$ m. The mixed *bending and torsion* vibration (case BT) was excited by a non-symmetrically applied, uniformly distributed, time harmonic line force in the x_2-direction at the free end $x_1 = L$. The force was *consistently distributed* over the free end surface in the bending case and consistently along the free edge $0 \leqslant x_2 \leqslant 1$, $x_3 = 0$ in the mixed bending–torsion case. In both cases, all displacements were constrained to zero at the fixed end $x_1 = 0$. No other constraints were imposed. For the symmetric bending case (B) two damping cases, normal strain damping

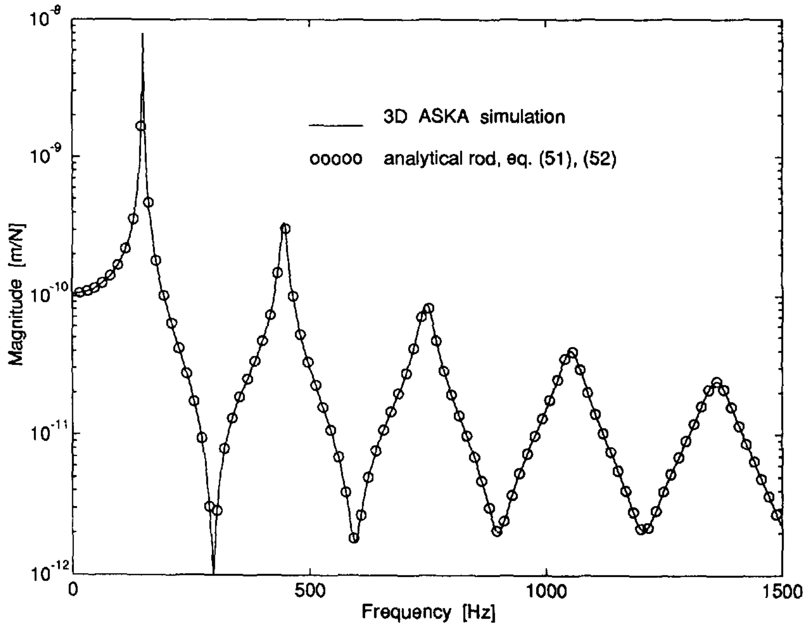

Fig. 2. End-displacement (receptance) of a longitudinally vibrating cantilever rod excited in the axial x-direction by a time harmonic unit force at the free end. Comparison between analytical solution (circles) and three-dimensional finite element simulation (solid line).

($\mu = 0$) and mixed $\varphi\mu$-damping ($\varphi \neq 0$, $\mu \neq 0$), were studied. For the non-symmetric, mixed bending-torsion case (BT) mixed $\varphi\mu$-damping was studied.

The elastic parameters and the mass density in the calculations were chosen to be (representative for aluminium):

$$\text{Young's modulus} \quad E_Y = 7.13\cdot 10^{10}\ \text{N m}^{-2}$$
$$\text{Poisson's ratio} \quad \nu = 0.3$$
$$\text{mass density} \quad \rho = 2750\ \text{kg m}^{-3}.$$

The damping parameters, corresponding to the isotropic augmented Hooke's law matrix (46) with one process l, were chosen as (cf. Section 8 above):

$$\varphi = 4.7766\cdot 10^{6}\ \text{N m}^{-2} \quad \mu = 0$$
$$\alpha = 8000\ \text{N m}^{-2}$$
$$\beta = 8000\ \text{rad s}^{-1},$$

in the normal strain φ-damping case *without* shear damping and as:

$$\varphi = 4.7766\cdot 10^{6}\ \text{N m}^{-2} \quad \mu = \varphi$$
$$\alpha = 8000\ \text{N m}^{-2}$$
$$\beta = 8000\ \text{rad s}^{-1}$$

in the *mixed* damping case with *both normal and shear strain damping*.

The results of the three-dimensional ASKA calculations are presented in Figs 3 and 4. The ASKA computations are compared to corresponding data (dotted line) for an analytic, plane Euler beam with the same geometry as the ASKA model and with a complex,

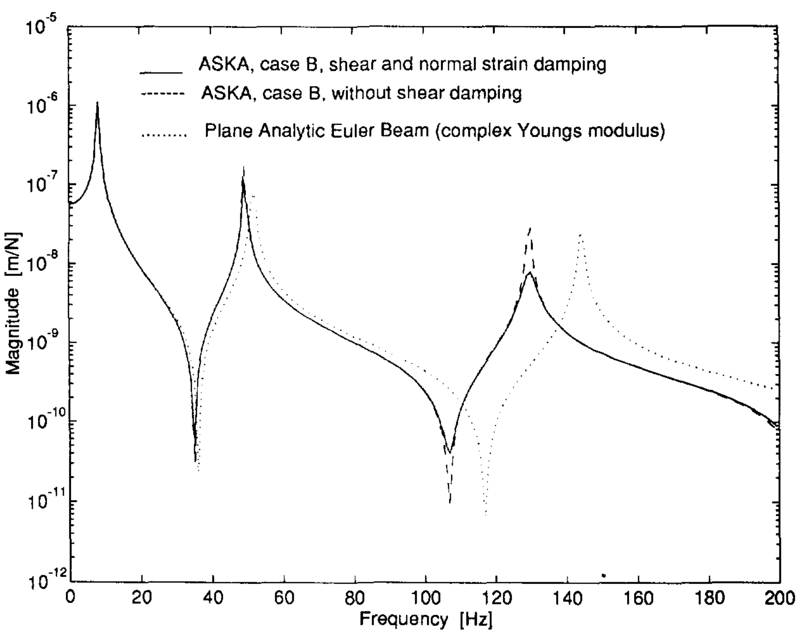

Fig. 3. Transverse, vertical, end-displacement u_2 (receptance) of cantilever beam, symmetrically excited (case B) in the transverse (vertical) x_2-direction by a time harmonic unit force at the free end. Mixed shear and normal strain damping (solid line) and normal strain damping only (dashed line). Comparison with plane analytical Euler beam (dotted line). Response point P, 0.1 m below the neutral layer.

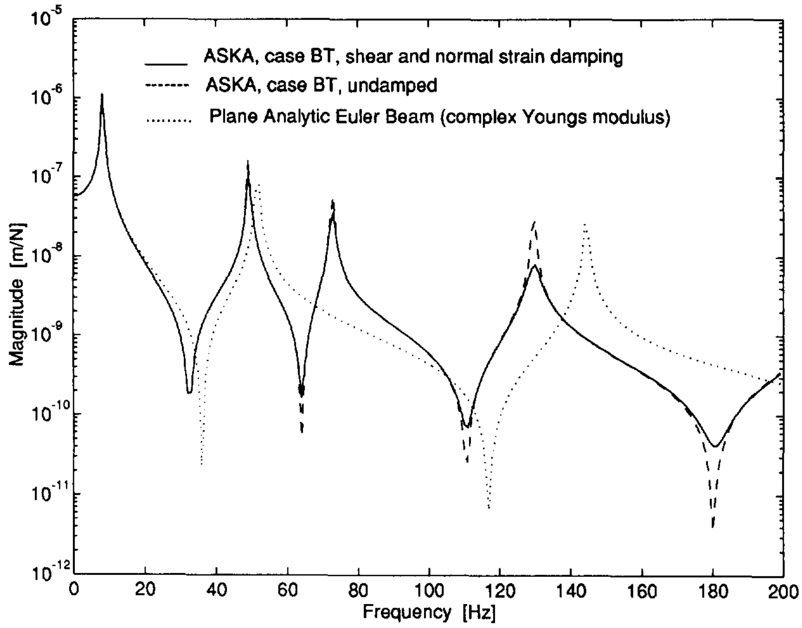

Fig. 4. Transverse, vertical, end-displacement u_2 (receptance) of cantilever beam, non-symmetrically excited (case BT) in the transverse (vertical) x_2-direction by a time harmonic unit force at the free end. Undamped (dashed line) and mixed shear and normal strain damping (solid line). Comparison with plane analytical Euler beam (dotted line). Response point Q at corner.

frequency dependent "Young's" modulus, defined by eqn (50), with $\delta = \varphi$ and the same α and β as above.

The *receptances*, i.e. magnitudes of frequency domain displacements $\tilde{u}_2$ divided by the excitation force at each frequency, presented in Figs 3 and 4, correspond to displacement responses at the point P ($x_1 = 10$ m, $x_2 = 0.4$ m, $x_3 = 0.5$ m) in the symmetric bending cases (B) and at the point Q ($x_1 = 10$ m, $x_2 = 1.0$ m, $x_3 = 0$ m) in the mixed bending–torsion cases (BT). The point P, thus, is situated 0.1 m below the neutral layer of the cantilever beam while the point Q is situated at a corner of the free end.

As may be seen in Figs 3 and 4, shear deformation of the cross-section contributes to the response already for frequencies around the second (bending) resonance. This can be concluded from the difference between the ASKA results and the curve for the plane Euler beam with its rigidly rotating cross-section (the Kirchhoff hypothesis).

It should also be noted that the magnitude of the third resonance peak in Fig. 3, at approximately 130 Hz, is lowered by a factor of about 3.8, compared to the case without shear damping ($\mu = 0$, dashed line), when the coupling parameter μ and thus shear damping is switched on (coupling parameter $\mu = \varphi > 0$).

In Fig. 4 the undamped non-symmetric bending case (BT), i.e. including torsion, is compared to the corresponding case with mixed damping. The third peak in Fig. 4 corresponds to the first torsional vibration mode of the cantilever and, as expected, the magnitudes of the first, second and third peak in Fig. 3 (mixed damping) are the same as the magnitudes of the first, second and fourth peak in Fig. 4.

SUMMARY

An isothermal, fully three-dimensional material damping modelling technique has been proposed. The method is formulated in the frequency domain and material damping is introduced in the constitutive equations by adding frequency dependent, complex valued terms to the classical material modulus matrix of Hooke's generalized law.

The derivations of this augmented Hooke's law (AHL) are based on linear, irreversible thermodynamics and the concept of augmenting thermodynamic fields used as hidden coordinates. A free energy density function, depending explicitly on the current infinitesimal strain and the thermodynamic, hidden variables, has been used as the time domain basis of the augmented Hooke's law. Through a time-domain model of the coupled evolution of the mechanical displacements and the thermodynamical variables, issues of causality are avoided completely in the final frequency domain formulation.

An isotropic augmented Hooke's law with both dilatational and shearing damping has been implemented and tested using a 20-node finite volume element. A close agreement between finite element calculations and the corresponding analytically exact results for the studied rod and beam cases was obtained.

Acknowledgements—This work was performed under contracts from the Swedish Defence Material Administration (Contract No. 23250-93-102-24-001) and the Commission of the European Communities (CEC) within the BRAIN (Basic Research in Aircraft Interior Noise) project (BRITE/AERO Contract 92-0032). The participation of FFA in the BRAIN project was funded by NUTEK (The National Board for Industrial and Technical Development), Sweden. The funding provided is gratefully acknowledged. Many thanks to Magnus Alvelid, ABB Traction, for introducing the author to the concept of augmenting thermodynamic fields and to Peter Göransson (manager of the BRAIN project) and Adam Zdunek, both at FFA, for valuable discussions and hints. Thanks, also, to Peter Göransson for doing the ASKA Acoustics implementation. The author gratefully acknowledges Saab Scania AB for the possibility to implement AHL in their ASKA finite element code at FFA. Acknowledgements also to Antonio Concilio, CIRA Italy, for interesting discussions concerning augmenting fields and the augmented Hooke's law.

REFERENCES

Bagley, R. L. and Torvik, P. J. (1983). Fractional calculus—a different approach to the analysis of viscoelastically damped structures. *AIAA J.* **21,** 741–748.

Bert, C. W. (1973). Material damping: an introductory review of mathematical models, measures, and experimental techniques. *J. Sound Vibr.* **29,** 129–153.

Biot, M. A. (1954). Theory of stress-strain relations in anisotropic viscoelasticity and relaxation phenomena. *J. Appl. Phys.* **25,** 1385–1391.

Biot, M. A. (1955). Variational principles in irreversible thermodynamics with application to viscoelasticity. *Phys. Rev.* **97,** 1463–1469.

Biot, M. A. (1956). Thermoelasticity and irreversible thermodynamics. *J. Appl. Phys.* **27,** 240–253.

Biot, M. A. (1958). Linear thermodynamics and the mechanics of solids. *Proc. Third U.S. Natl Congr. Appl. Mech.*, 1–18.

Biot, M. A. (1959). New thermomechanical reciprocity relations with application to thermal stress analysis. *J. Aero/Space Sci.* **26,** 401–408.

Ewins, D. J. (1986). *Modal Testing: Theory and Practice*. Research Studies Press and Brüel & Kjaer.

Fung, Y. C. (1965). *Foundation of Solid Mechanics*. Prentice-Hall, London.

Golla, D. F. and Hughes, P. C. (1985). Dynamics of viscoelastic structures—a time domain, finite element formulation. *J. Appl. Mech.* **52,** 897–906.

Göransson, P. (1988). *ASKA Acoustics. Theory and Applications*. FFA TN 1988–13. The Aeronautical Research Institute of Sweden, Stockholm.

de Groot, S. R. and Mazur, P. (1962). *Non-equilibrium Thermodynamics*. North-Holland, Amsterdam.

Kinra, V. K. and Wolfenden, A. (eds) (1992). *M³D: Mechanics and Mechanisms of Material Damping*, ASTM STP 1169. American Society for Testing and Materials, Philadelphia.

Lesieutre, G. A. (1989). Finite element modelling of frequency-dependent material damping using augmenting thermodynamic fields. Ph. D. dissertation. Aerospace Engineering, University of California, Los Angeles.

Lesieutre, G. A. (1992a). Finite elements for dynamic modelling of uniaxial rods with frequency-dependent material properties. *Int. J. Solids Structures* **29,** 1567–1579.

Lesieutre, G. A. (1992b). Finite elements for modeling frequency dependent material damping using internal state variables. American Society for Testing and Materials ASTM STP 1169, 344–357.

Lesieutre, G. A. and Bianchini, E. (1993). Time domain modeling of linear viscoelasticity using augmenting thermodynamic fields. *Proc. 34th AIAA/ASME/ASCE/AHS/ASC Structures, Structural Dynam. Mater. Conf.* La Jolla, CA, 2101–2109.

Lesieutre, G. A. and Govindswamy, K. (1994). Modeling temperature- and frequency-dependent dynamic behavior of viscoelastic structures using anelastic displacement fields. *Proc. 34th AIAA/ASME/ASCE/AHS/ASC Structures, Structural Dynam. Mater. Conf.* Hilton Head, SC, 2691–2700.

Lesieutre, G. A. and Mingori, D. L. (1990). Finite element modelling of frequency-dependent material damping using augmenting thermodynamic fields. *J. Guidance Cont., Dynam.* **13,** 1040–1050.

McTavish, D. J. and Hughes, P. C. (1993). Modeling of linear viscoelastic space structures. *J. Vibration Acoustics* **115,** 103–110.

Nashif, A. D., Jones, D. I. G. and Henderson, J. P. (1985). *Vibration Damping*. John Wiley, New York.

Nowick, A. S. and Berry, B. S. (1972). *Anelastic Relaxation in Crystalline Solids*. Academic Press, New York.

Reddy, J. N. (1986). *Applied Functional Analysis and Variational Methods in Engineering*. McGraw-Hill, New York.

Ruzicka, J. E. (ed.) (1960) Structural damping. Papers presented at a colloquium on structural damping. ASME annual meeting, Atlantic City, N. J., 1959. Pergamon Press, Oxford.

Truesdell, C. and Noll, W. (1992). *The Non-linear Field Theories of Mechanics*. 2nd Edn. Springer, Berlin.

Yiu, Y. C. (1993). Finite element analysis of structures with classical viscoelastic materials. *Proc. 34th AIAA/ASME/ASCE/AHS/ASC Structures, Structural Dynam. Mater. Conf.* La Jolla, CA, 2110–2119.

APPENDIX

The matrix fields (column vectors) u, σ and E are defined as:

$$u = u(\mathbf{x}, t) = [u_1 \quad u_2 \quad u_3]^{\mathrm{T}} \tag{A1}$$

$$\sigma = \sigma(\mathbf{x}, t) = [\sigma_{11} \quad \sigma_{22} \quad \sigma_{33} \quad \sigma_{12} \quad \sigma_{23} \quad \sigma_{31}]^{\mathrm{T}} \tag{A2}$$

$$E = E(\mathbf{x}, t) = [\varepsilon_{11} \quad \varepsilon_{22} \quad \varepsilon_{33} \quad 2\varepsilon_{12} \quad 2\varepsilon_{23} \quad 2\varepsilon_{31}]^{\mathrm{T}}, \tag{A3}$$

where u_i, σ_{ik} and ε_{ik} are Cartesian vector and tensor components. Thus σ and E, respectively, are six-dimensional, Cartesian matrix representations of the symmetric stress tensor and the symmetric (infinitesimal) strain tensor.

The divergence $div(\mathbf{S})$ of the stress tensor $\mathbf{S}$, in Cartesian matrix notation, may be represented by the three-dimensional matrix field $\mathbf{D}^{\mathrm{T}}[\sigma]$ where $\mathbf{D}^{\mathrm{T}}$ is the first order, spatial, partial differential operator matrix:

$$\mathbf{D}^{\mathrm{T}} = \mathbf{D}^{\mathrm{T}}[\ ] \equiv \begin{bmatrix} \frac{\partial}{\partial x_1} & 0 & 0 & \frac{\partial}{\partial x_2} & 0 & \frac{\partial}{\partial x_3} \\ 0 & \frac{\partial}{\partial x_2} & 0 & \frac{\partial}{\partial x_1} & \frac{\partial}{\partial x_3} & 0 \\ 0 & 0 & \frac{\partial}{\partial x_3} & 0 & \frac{\partial}{\partial x_2} & \frac{\partial}{\partial x_1} \end{bmatrix}. \tag{A4}$$

The matrix operator $\mathbf{D}^{\mathrm{T}}$ is uniquely defined provided that:

$$\mathbf{u} \cdot div(\mathbf{S}) \equiv u^{\mathrm{T}}\mathbf{D}^{\mathrm{T}}[\sigma] \tag{A5}$$

for all (displacement) vector fields $\mathbf{u}$ and second order (stress) tensor fields $\mathbf{S}$ with Cartesian matrix representations u and σ, respectively.

The strain vector E, also called the engineering strain vector, may be determined from the three displacement components u_i as:

$$E = \mathbf{D}[u], \tag{A6}$$

where the first order, spatial, partial differential operator matrix $\mathbf{D}$ is identical to the matrix transpose of the operator matrix $\mathbf{D}^{\mathrm{T}}$ defined in matrix (A4).